Adv. Geosci., 11, 21–29, 2007
www.adv-geosci.net/11/21/2007/

Advances in Geosciences

Quasi 2D hydrodynamic modelling of the flooded hinterland due to dyke breaching on the Elbe River

S. Huang, S. Vorogushyn, and K.-E. Lindenschmidt

GFZ GeoForschungsZentrum Potsdam, Section 5.4 – Engineering, Hydrology, Telegrafenberg, 14473 Potsdam, Germany

Received: 15 December 2006 – Revised: 5 April 2007 – Accepted: 4 May 2007 – Published: 16 May 2007

Abstract. In flood modeling, many 1D and 2D combination and 2D models are used to simulate diversion of water from rivers through dyke breaches into the hinterland for extreme flood events. However, these models are too demanding in data requirements and computational resources which is an important consideration when uncertainty analysis using Monte Carlo techniques is used to complement the modeling exercise. The goal of this paper is to show the development of a quasi-2D modeling approach, which still calculates the dynamic wave in 1D but the discretisation of the computational units are in 2D, allowing a better spatial representation of the flow in the hinterland due to dyke breaching without a large additional expenditure on data preprocessing and computational time. A 2D representation of the flow and velocity fields is required to model sediment and micro-pollutant transport. The model DYNHYD (1D hydrodynamics) from the WASP5 modeling package was used as a basis for the simulations. The model was extended to incorporate the quasi-2D approach and a Monte-Carlo Analysis was used to conduct a flood sensitivity analysis to determine the sensitivity of parameters and boundary conditions to the resulting water flow. An extreme flood event on the Elbe River, Germany, with a possible dyke breach area was used as a test case. The results show a good similarity with those obtained from another 1D/2D modeling study.

1 Introduction

Hydrodynamic models are important for the simulation and prediction of inundation processes due to dyke breaching during flood events. An array of models of varying complexity levels may be used. Following a categorization in the number of spatial dimensions, simulations are often carried out using one-dimensional (1D) or two-dimensional (2D) models. 1D hydrodynamic models often solve the St.Venant full dynamic wave equations which respect to both momentum and mass continuity of water transport through a meshed system. 2D models are based on shallow water equations to describe the motion of water (for examples, see D'Alpaos et al., 1994 and Chua et al., 2001). A combination of both 1D and 2D approaches have also been used in which the flow in the main river channel is solved in 1D and the overbank inundated areas are solved in 2D using the diffusive wave equation or storage cells (for examples, see Bates and De Roo, 2000; Han et al., 1998 and Vorogushyn et al., 2007). 2D and 1D/2D combination models are generally computationally more extensive and have more requirements on input data and pre-processing than 1D models. This is particularly a concern when automated methods for parameter optimization or Monte-Carlo methods for uncertainty analysis are to be implemented. However, 1D models are not sufficient to describe the spatial variability of water depths, velocities and flows in floodplains, polders and other overbanked inundated areas during flood events.

Hence, a quasi-2D approach using a 1D hydrodynamic model is proposed that allows its discretisation to be extended into the hinterland giving a 2D representation of the inundation area (see Fig. 1). Aureli et al. (2006) have used quasi-2D numerical modeling adopting the hydrodynamic module of the software DHI-Mike 11. We also compared the results of a dyke breach and hinterland inundation obtained from a quasi-2D model and a fully-2D finite volume model and found good agreement between them in the simulation results.

In this study, the quasi-2D approach can be achieved with the model DYNHYD, which is part of the WASP5 (Water Quality Analysis Simulation Program) package developed by the U.S. Environmental Protection Agency (Ambrose et al., 1993). DYNHYD solves the 1D equation of continuity and momentum for a branching or channel-junction (link-node)

Correspondence to: K.-E. Lindenschmidt
(kel@gfz-potsdam.de)

Published by Copernicus Publications on behalf of the European Geosciences Union.

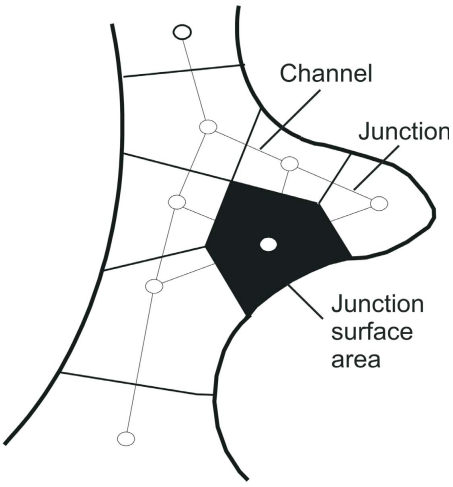

Fig. 1. 1D hydrodynamic channel-junction (link-node) network allowing a 2D spatial representation of overbank inundated areas (source: Ambrose et al., 1993).

Table 1. Discharge statistics for the gages at Torgau and Lutherstadt Wittenberg (MQ – mean discharge, MHQ – mean maximum annual flood, HQ – highest recorded flood event); source: Gewässerkündliches Jahrbuch, Elbegebiet Teil 1, 2003.

			Discharge (m^3/s)		
Gage	Elbe-km	Series	MQ	MHQ	HQ (date)
Torgau	154.2	1936 - 2003	344	1420	4420 (18.08.2002)
L. Wittenberg	214.1	1961 - 2003	369	1410	4120 (18.08.2002)

computational network. This model is discretised to the hinterland representing the inundation area. Monte-Carlo Analyses were carried out to analyze globally the sensitivity of selected parameters and boundary conditions on state variables. The analysis also indicates good model stability for a wider range of parameter settings and boundary conditions and the model's applicability to other test sites.

2 Methods

2.1 Hydrodynamic model DYNHYD

This description of the model DYNHYD has been drawn from Ambrose et al. (1993), Lindenschmidt et al. (2005) and Lindenschmidt (2007)[1], however, a short excerpt is warranted here. In DYNHYD a river is discretised using a "channel-junction" scheme. The channels have rectangular cross-sections and calculate the transport of water by the equations of motion:

$$\frac{\partial U}{\partial t} = -U\frac{\partial U}{\partial x} + a_g + a_f \tag{1}$$

where a_f is the frictional acceleration, a_g is the gravitational acceleration along the longitudinal axis x, U is the mean velocity, $\partial U/\partial t$ is the local inertia term, or the velocity rate of change with respect to time t and $U\partial U/\partial x$ is the convective inertia term, or the rate of momentum change by mass transfer. The junctions calculate the storage of water described by the continuity equation:

$$\frac{\partial H}{\partial t} = \frac{1}{B}\cdot\frac{\partial Q}{\partial x} \tag{2}$$

where B is the channel width, H is the water surface elevation (head), $\partial H/\partial t$ is the rate of water surface elevation change with respect to time t, and $\partial Q/\partial x$ is the rate of water volume change with respect to distance x. The discharge Q is additionally related to river morphology and bottom roughness using Manning's equation:

$$Q = \frac{r_H^{2/3}\cdot A}{n}\sqrt{\frac{\partial H}{\partial x}} \tag{3}$$

where A is the cross-sectional area of the water flow, n is the roughness coefficient of the river bed, r_H is the hydraulic radius and $\partial H/\partial x$ is the slope of the river bed in the longitudinal direction x. Discharge over a weir is calculated by the weir equation:

$$Q = \alpha\cdot b\cdot h^{1.5} \tag{4}$$

where α is the weir coefficient, b is the weir breadth and h is the depth between the upstream water level and the weir crest. Backwater effects were also taken into consideration using a submerged weir formula.

2.2 Adaptations to DYNYHD for quasi-2D flood modelling

In this algorithm the inlet and outlet discharges of a dyke are controlled by a "virtual" weir. This algorithm was first developed for floodplains (see Lindenschmidt, 2007[1]; Lindenschmidt et al., 2006) and polders (see Huang et al., 2007) and has been extended here for dyke breach areas. Due to the condition of water continuity and stability requirements water levels in the discretisation elements cannot fall dry, hence an extension to the model was implemented to capture the flooding and emptying of the hinterland during a flood simulation. During low flows when dyke breaching does not occur a small amount of water is allowed to leak through the weir from the river into the hinterland to prevent the discretised elements depicting the hinterland from becoming dry. This volume is very minute compared to the discharge in the river so that the error in the simulations is insignificant. To simulate a dyke breach, the weir is opened by lowering the weir crest to the level of the hinterland ground level.

[1]Lindenschmidt, K.-E.: Quasi-2D approach in modelling the transport of contaminated sediments in floodplains during river flooding – model coupling and uncertainty analysis, Environmental Engineering Sciences, in review, 2007.

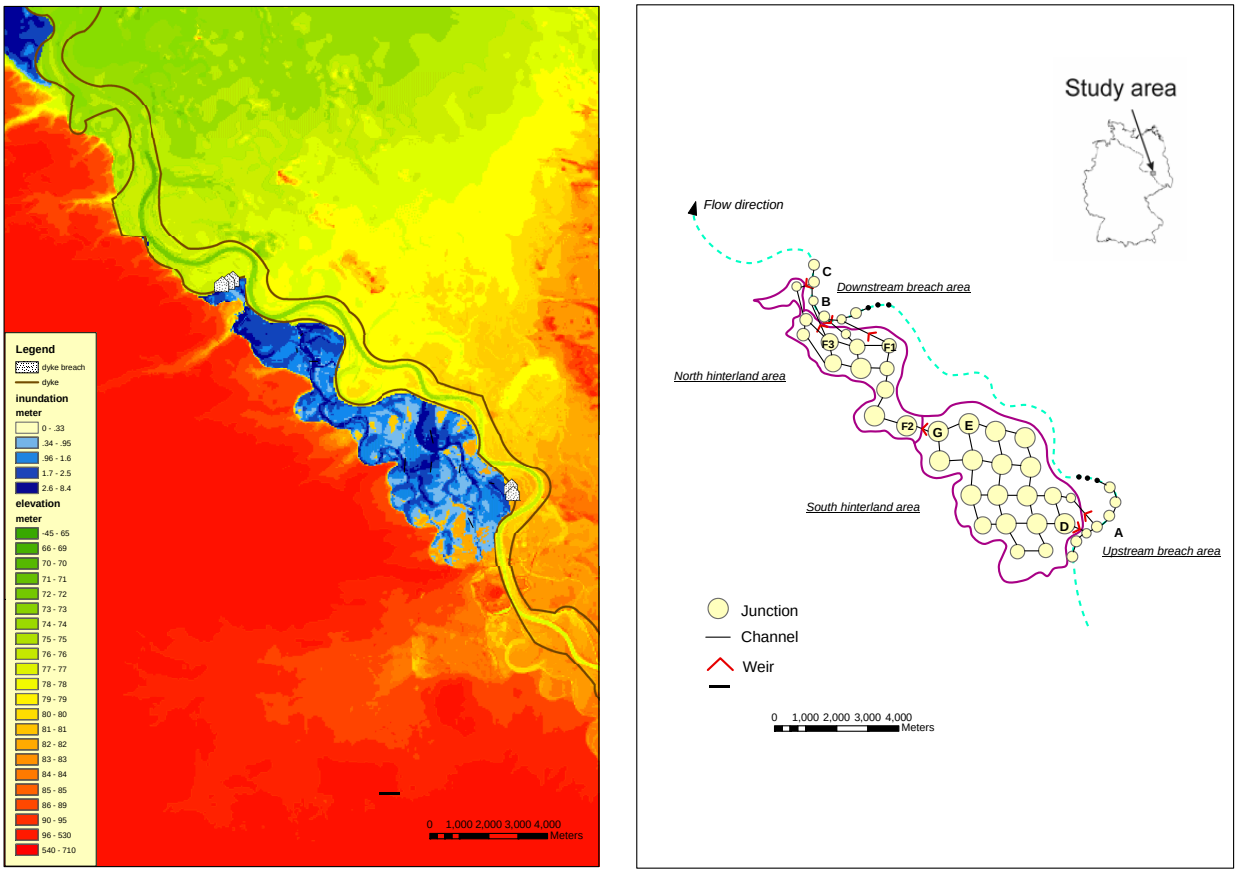

Fig. 2. The study area and the inundation hinterland **(a)** and the discretisation with junctions and channels of the studied hinterland **(b)**.

3 Study site and model setup

The study site is the middle course of the Elbe River in Germany between the gages at Torgau (Elbe-km 154.2) and Lutherstadt Wittenberg (Elbe-km 214.1). This stretch of the river is heavily modified with dykes running along both sides for most of the flow distance. Characteristics of the discharges recorded at the gages at Torgau and Lutherstadt Wittenberg are given in Table 1. Dyke breaching only between Elbe-km 154.2 and Elbe-km 192 was considered for the modeling exercise. There are no major tributaries flowing into the Elbe in this reach. High water level readings and the water level readings from the gage at Mauken (at Elbe-km 184.5) were used to compare measurements with hydrodynamic simulations. Model calibration and validation was carried out in another study (Lindenschmidt and Huang, 2007[2]) with data from flood events in which breaching did not occur. Data from the Torgau gage during the most severe flood recorded (August 2002) was used as a boundary condition. The information on dyke breaches and the inundation area was drawn from the results of the 1D/2D simulation in this area (Vorogushyn et al., 2007). This model consists of a 1D hydrodynamic (St. Venant equation) model for the Elbe River, a dyke breach model to predict dyke breaching and a 2D storage-cell model for the simulation of inundation behind the dyke in the hinterland. The dyke breach model simulated the breach locations due to overtopping based on the approach of Apel et al. (2004). From the results of this model, the dykes around Elbe-km 158 (upstream breach area) and between Elbe-km 173 and 179 (downstream breach area) are prone to breaching and the inundation area is shown in Fig. 2a. This model was used for comparison with simulations in this study and to test the performance of the quasi-2D modeling approach.

3.1 Input data

The model of the river reach was set up on the basis of cross-sectional profiles available every 500 m along the river from which initial hydraulic radii and segment water volumes were derived. The time frame of the modeled flow event is 13–22 August 2002, and the discharge recordings

[2]Lindenschmidt, K.-E. and Huang, S.: Simulating sediment and micro-pollutant transport in polder systems using a quasi-2D flood model, in preparation, 2007.

from the Torgau gage were used for the upper boundary condition of the hydrodynamic model.

3.2 Discretisation

The discretisation of channels and junctions with inlet and outlet weirs is shown for the river and inundated hinterland in Fig. 2b. There are three pairs of weirs set for the simulation of breaches. Each pair constituents an inlet and an outlet for water flow. The inlet weir controls the water flowing into the hinterland and the outlet weir is used to simulate the back water after the flood peak in the river has passed and water flows from the hinterland back into the river. The first pair of weirs, which are near the river section A shown in Fig. 2b, represent the breaches on the upstream portion of the reach around Elbe-km 158 on the fourth day of the simulation. The breaches on the downstream portion of the studied reach (between Elbe-km 173 and 179) were simulated by another two pairs of weirs near the river channel B and C, which eroded on the first and third simulation days, respectively. There is another weir set between the two parts of the hinterland to compensate for the difference in the average elevation of the hinterland land surfaces between these two parts (an average of 77.5 m and 79.5 m was calculated from a 50 m resolution digital elevation model for the northern and southern parts, respectively).

The simulation results are output on an hourly time step. A longitudinal profile of the maximum water level attained during the flood and the water level hydrograph recorded at Mauken (Elbe-km 184.5) were available for testing of the hydrodynamic model.

3.3 Local sensitivity analysis

Prior to the Monte-Carlo analysis, a sensitivity analysis was carried out to check the response of the system by varying different parameters. The parameters include:

1. Weir coefficient α from the weir discharge equation. The percentage deviations in α may also represent the percentage deviation in weir breadth b, since both are multiplicative values in the weir equation. Only α was used in the MOCA due to the linear compensatory effect of α and b on output variables (e.g. a 10% increase in α can be compensated by a 10% decrease in b).

2. Roughness coefficient n of the channel bed from Manning's equation

3. Percentage deviations in the discharge boundary condition q at the Torgau gage

The elasticity ε was used to quantify the local sensitivity of the input parameters:

$$\varepsilon = \frac{\partial O}{\partial P} \cdot \frac{P}{O} \tag{5}$$

where: O = model output value; P = input parameter value. A base simulation is first run, with result O_{base}, using a base parameter value P_{base}, after which the parameter is then increased by a certain fraction x designed as P_x which gives the result O_x. The elasticity then becomes:

$$\varepsilon \approx \frac{\Delta O}{\Delta P} \cdot \frac{P}{O} = \frac{(O_x - O_{\text{base}})}{(P_x - P_{\text{base}})} \cdot \frac{P_{\text{base}}}{O_{\text{base}}} \tag{6}$$

Since $P_x{=}(1{+}x){\cdot}P_{\text{base}}$ the equation reduces to:

$$\varepsilon = \frac{1}{x}\left(\frac{O_x - O_{\text{base}}}{O_{\text{base}}}\right) \tag{7}$$

An elasticity value is calculated for each parameter used, which were increased by 10% separately for each single run. Hence, x equals 0.1 and the equation reduces to:

$$\varepsilon = 10 \cdot \left(\frac{O_x - O_{\text{base}}}{O_{\text{base}}}\right) \tag{8}$$

3.4 Global sensitivity analysis

Global sensitivity analysis apportions the output uncertainty to the uncertainty in the input factors, described typically by probability distribution functions that cover the factors' range of existence (Saltelli et al., 2000). Here, the results from a Monte Carlo Analysis of 1000 model runs were analyzed to see the co-relationship among those variables and their contributions to the result. For the MOCA, the modeling system was run 1000 times for which a new set of values for the parameters were generated randomly from normal probability distributions for each simulation run. A final MOCA was carried out in which all of the parameters were varied together to see the total effects on the output distribution after 1000 simulations.

The parameters α, n and q were incremented or decremented within a $\pm$10% deviation range. Then values were selected from normal distributions with ranges 1.17 to 1.43 for α, 0.034 to 0.042 for n (variation of roughness coefficients in hinterland calculated for different land-use types, see Vorogushyn et al., 2007) and -0.1 to 0.1 for q (typical error range for discharge measurements, see Herschy, 1995; Lindenschmidt et al., 2005). Figure 3 shows the hydrograph used at the boundary condition at Torgau. The box-whisker plots illustrate the $\pm$10% deviations used in the discharge values for the MOCA. Note that the range of deviations increases with larger discharges.

To better interpret the behavior of uncertainty propagation through the modeling process and the contribution of the error of each input value to the overall uncertainty in the model predictive outcome, the coefficient of variation CV was used to standardize the input and output normal distributions for comparison of the MOCA results:

$$CV = \frac{\text{Standard deviation}}{\text{mean}} \tag{9}$$

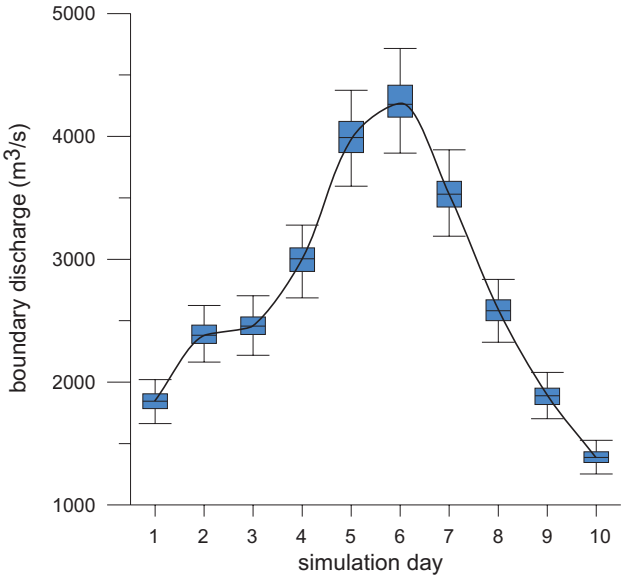

Fig. 3. Hydrograph of boundary condition at Torgau with box-whisker plots indicating the range in the discharge deviation, which depict the minimum, maximum, medium and lower and upper quartiles of each sample group.

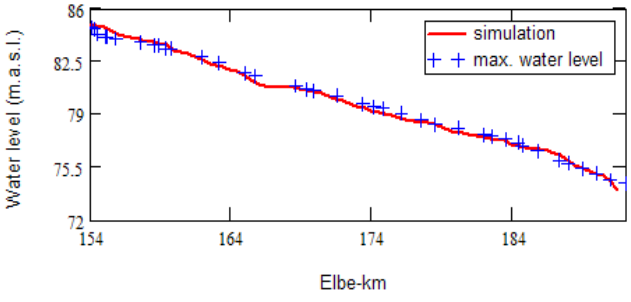

Fig. 4. Longitudinal profile of simulation day 5.2 and the high water marks, indicating the maximum water level attained.

4 Results and discussion

4.1 Hydrograph simulations

The first step in the model adaptation was to model the actual conditions of the August 2002 flood. A longitudinal profile of measured maximum water levels attained during this flood event was available for comparison of the hydrodynamic model results. Figure 4 shows good agreement between the simulated profiles at a simulation time of 5.2 days. The Manning's roughness coefficient between 0.030 to 0.040 $s/m^{1/3}$ provided the best fit of the simulations to the data. This value is somewhat higher than the one of 0.025 $s/m^{1/3}$ calibrated for the 1D/2D simulation by Vorogushyn et al. (2007). The water levels recorded at the gage at Mauken provided temporal data for a comparison between measurements and simulation results which shows a good fit in Fig. 5. The simulations are somewhat overestimated, because the diversion of water due to dyke breaching is not included.

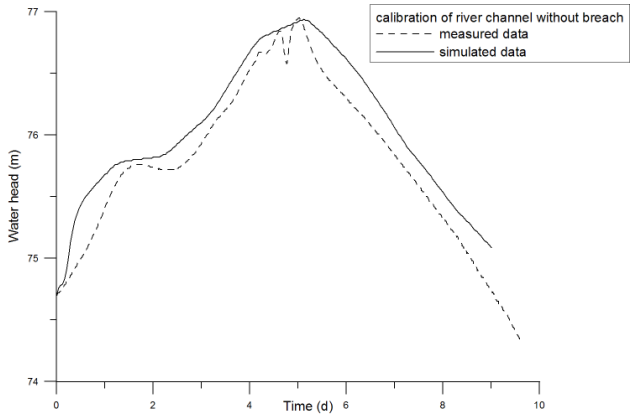

Fig. 5. Measured and simulated water levels at the gage Mauken.

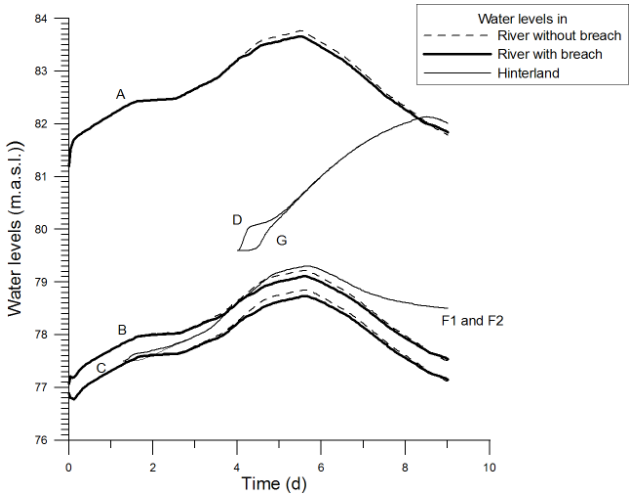

Fig. 6. Water levels in the river and hinterland. See Fig. 2b for locations A to G.

4.2 Dyke breach

Figure 6 shows the simulated water heads in the hinterland and the adjacent river sections. It presents a plausible water flow behavior in the hinterland and capping of the discharge hydrograph in the main river channel. The difference in the filling times of the flood waters traveling between locations D and G (refer to Fig. 2b) illustrates the spatial differentiation that can be obtained using the quasi-2D approach. The travel time of the water through the south hinterland area between points D and G is approximately 7 h, while through the north hinterland area between points F3 and F2 it is 6 h after the downstream dyke breaches. Vorogushyn et al. (2007) give flood depths of the hinterland in every 12 h increments

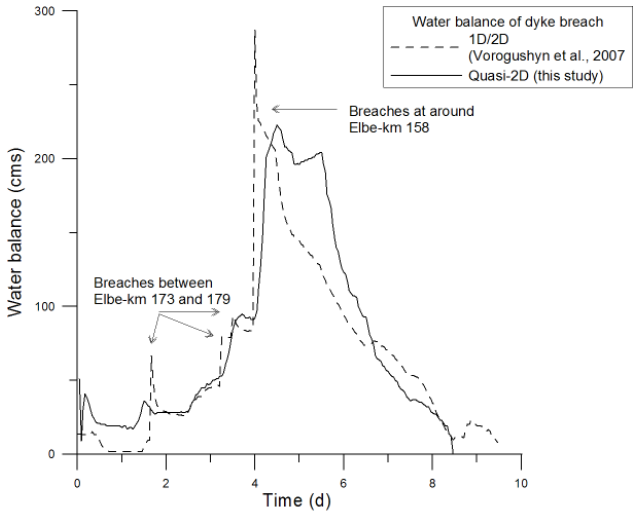

Fig. 7. Comparison of water balances for upstream and downstream dyke breaches between the 1D/2D modelling and quasi-2D modelling.

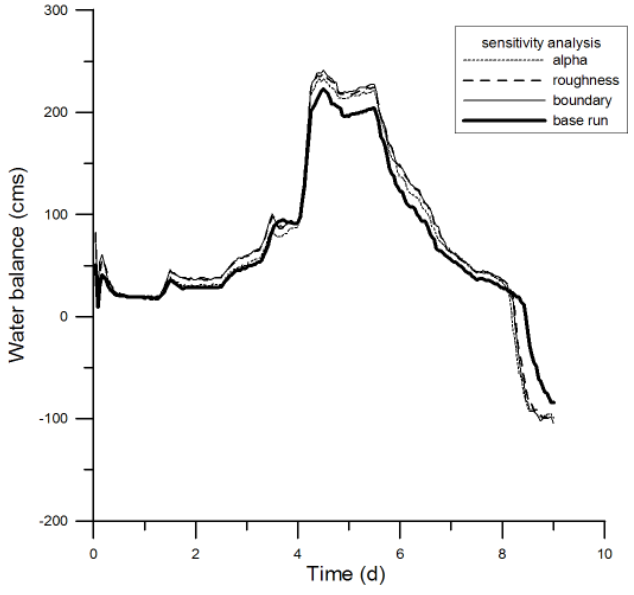

Fig. 8. The total water balance in the hinterland when each parameter was increased by 10% for the entire reach with breaching dykes.

and it is found that the water can only reach G after breaching in 36 h and F2 in 48 h. Hence it is obvious that the water travels faster in the quasi-2D model which may be due to the lower roughness values used for the hinterland surfaces and the averaging of the terrain elevations in the two hinterland areas. To compare the result, the water balances between the upstream and downstream breaches, which indicate how much water is flowing through the breaches into the hinterland, were calculated for each modeling approach (see Fig. 7). The flow through the most upstream breach on Day 4 seems very abrupt for the 1D/2D model. Erosion of the dyke

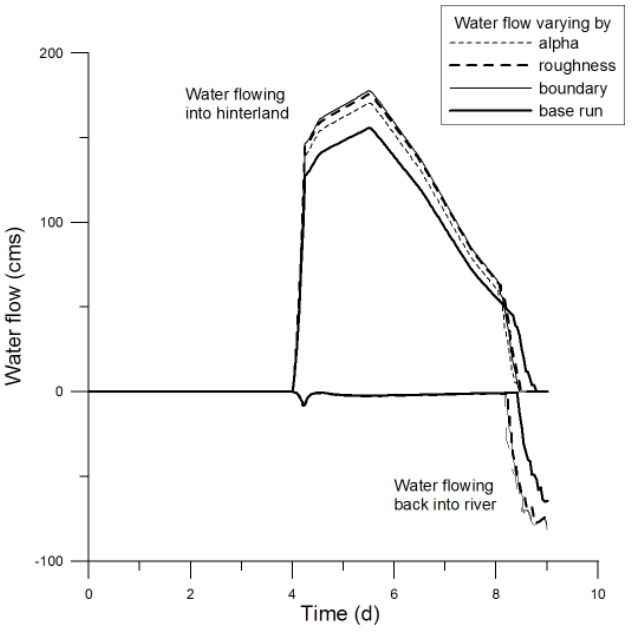

Fig. 9. Water flowing through the upstream breaches at Elbe-km 158 when each parameter is increased by 10%.

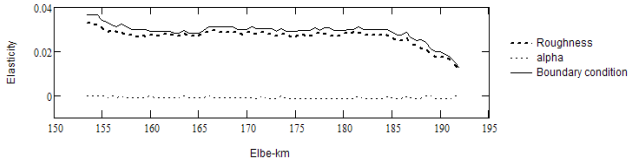

Fig. 10. Elasticity analysis for the river channel; parameter sensitivity on water level.

for the 1D/2D model is an instantaneous process, whereas dyke erosion is allowed for in the quasi-2D model by successively lowering the weir crest over a six hour time frame. The flow behavior was similar for both modeling systems for the two most downstream dyke breaches during Day 1 and 3. The last breach occurred on Day 4 in the upstream breach area which leads to much more water flowing into the upper hinterland. The quasi-2D model simulated the back flow of water from the hinterland to the river more rapidly and earlier, which may also explain the rapid water flow through the hinterland.

4.3 Local sensitivity analysis

Figure 8 shows the water balance of the inundated areas from simulations, each with one parameter increased by 10%. The parameters q and n have a slightly larger sensitivity on the result than α but in general, all three parameters are relatively equally sensitive on the water balance of the river-hinterland system which justifies incorporating all three in the MOCA analysis.

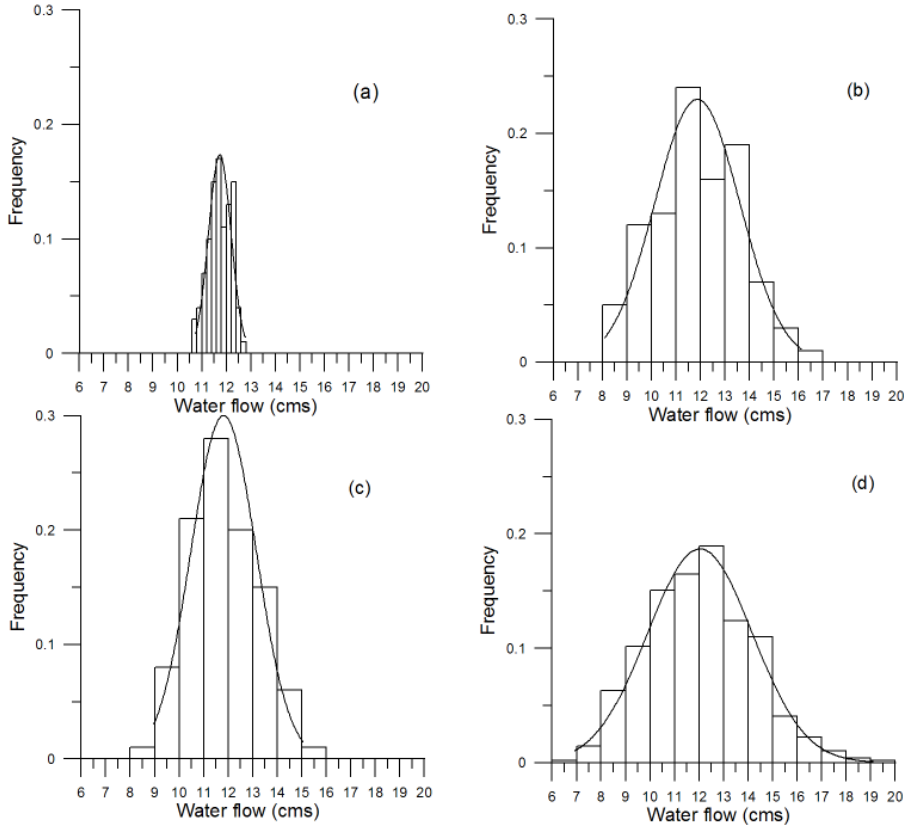

Fig. 11. Probability distribution of mean water flow during the first breach at F1 by varying alpha **(a)**, roughness **(b)**, boundary condition deviation **(c)** and all of these three parameters **(d)**.

The sensitivity of the three parameters on water flow through the dyke breaches is similar as on the water balance (see Fig. 9). For the upstream breach area, the most sensitive parameter is the deviation in the boundary conditions, next is roughness, and least important is α. These effects are also reflected in the elasticity analysis of each parameter on flow in the hinterland areas (data not shown). In this case, the elasticity remains fairly constant equaling about 1, which means a 10% increase of a parameter leads to a 10% increase in the result. It is also noticed that on the onset of water flow into or out of the hinterland, the elasticity on flow of each parameter varies greater than during other periods, and the outflow is much more sensitive to parameter change than the inflow because the hinterland fills faster and the water flows back to the river earlier.

In addition, the water head along the whole river channel was analyzed. The major parameters influencing the head are the roughness and boundary condition deviations, because the water volume in the hinterland is not significantly large compared to the river flow (see Fig. 10, which shows the elasticity along the river when all of the dyke breaches occurred).

4.4 Global sensitivity analysis

In this study, all the parameters α, n and q were used together in the Monte-Carlo analyses. Figure 11 shows the probability distributions of water flow at F1 (refer to Fig. 2b) by varying each parameter separately or all three together. The mean value of these distributions does not differ much, ranging from 11.8 to 12.0 cms. However, the three variables together can lead to a wider range in the distribution. Both roughness and the deviations in boundary conditions contribute more uncertainty (broader distribution) to the result than does the weir coefficient.

Figure 12 gives the CVs for each breach and the adjacent river channels. At all locations, there is an increasing trend in the CVs when all parameters are implemented in the MOCA. This is due to the increase in the number of varying parameters in the model which leads to an increased spread in the distributions of the simulated results. α influences the results the least in both hinterland and river channels. The boundary condition is the main factor affecting the water flow through the river-hinterland system in the main channel. Both n and q play important roles in controlling flow through the hinterland.

Table 2. The co-relationship between different parameters and the water flow. Refer to Fig. 2b for the location sites.

Locations	Coefficient of determination (r^2) (%)			
	α	n (hinterland)	n (river)	q
F1	7	<1	8	34
F3	11	<1	10	28
D	21	<1	45	30
A	2	<1	<1	95
B	<1	<1	<1	77
C	<1	<1	<1	90

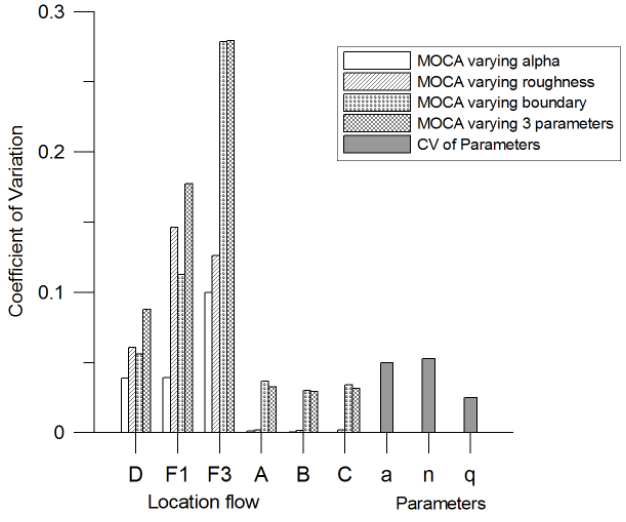

Fig. 12. Coefficient of variations for four different Monte Carlo analyses by varying: i) alpha only; ii) roughness only; iii) boundary condition only and iv) varying all three factors simultaneously.

The co-relationship between the parameters and resulting variables can be explored using plots of scattered dots with the parameter values plotted in the x-axis against the variable values on the y-axis (see examples in Fig. 13). All the MOCA runs were used in which α, n and q were varied. The slope of the line indicates how the parameter values correlate with their respective variable results. Figure 13a shows the scatter plots of the parameter α plotted with the corresponding value of water flow at location D. A linear regression was plotted from which the coefficient of determination r^2 was calculated. For the water flow in the southern hinterland area in the vicinity of the dyke breach, 21%, 45% and 30% (the latter not shown) of the total variation of the water flow values can be accounted for by a linear relationship with values of α, n, and q, respectively. Table 2 summarizes the total variation on water flow at different locations in the river-hinterland system. Only the roughness coefficient in the river correlates significantly with water flows. The roughness in the hinterland surfaces is not sensitive to the flows in the system since the flow through the dyke breaches is dominated by the weir and river discharges. It is obvious that the boundary condition is the most sensitive factor to the water volumes in river channels and the effects of weir discharge and bottom roughness are stronger in the hinterland, especially at the location D during the third breach. This is due to the high water level in the main channel at Day 4, so that h in the weir equation is very large.

5 Conclusion and outlook

Several conclusions can be drawn from this study:

1. The quasi-2D approach is applicable in capturing the flood dynamics of a river reach in which dyke breaching has occurred. The 2D representation allows future modeling studies of sediment transport to quantify sedimentation and re-suspension during filling and draining of the hinterland.

2. The water balance at breach locations from the quasi-2D modeling results compared well with those obtained from the 1D/2D model from Vorogushyn et al. (2007). Flood water travels faster in the quasi-2D model due to the lower values used for bottom roughness in the hinterland and due to the averaging of the hinterland surface elevations.

3. The uncertainty in the bottom roughness and the boundary conditions contribute more significantly to the uncertainty of flow characteristics throughout the river-hinterland system than the parameters controlling discharge through the dyke breach.

Further study based on this modeling exercise will focus on the uncertainty analysis of the parameters, but with different tools, such as SIMLAB, which is also designed for Monte-Carlo analysis. The water quality model TOXI will be added to simulate the transport and fate of sediments and heavy metals in the inundated areas. Furthermore, the polders in the river system will also be included to see the influence of dyke breaches and the polder control for peak discharge capping. Finally, this modeling section will be extended to the gage at Wittenberg to check the effects of hydrograph capping by dyke breaches and polder control on a larger scale.

Edited by: K.-E. Lindenschmidt
Reviewed by: P. Krause and H. Apel

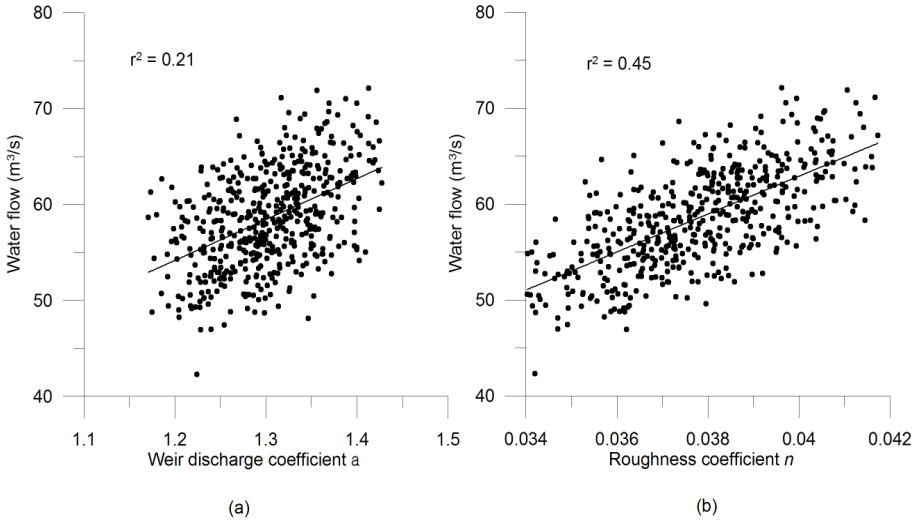

Fig. 13. Co-relationship between the river water flow at location D (y-axis) and **(a)** α, **(b)** n in the adjacent river reach.

References

Ambrose, R. B., Wool, T. A., and Martin, J. L.: The Water Quality Simulation Program, WASP5: model theory, user's manual, and programmer's guide, U.S. Environmental Protection Agency, Athens, GA, http://www.epa.gov/ceampubl/swater/wasp/, 1993.

Apel, H., Thieken, A., Merz, B., and Blöschl, G.: Flood risk assessment and associated uncertainty, Nat. Hazards Earth Syst. Sci., 4, 295–308, 2004, http://www.nat-hazards-earth-syst-sci.net/4/295/2004/.

Aureli, A., Maranzoni, A., Mignosa, P., and Ziveri, C.: Flood hazard mapping by means of filly-2D and quasi-2D numerical modeling: a case study, in: Floods, from defence to management, edited by: van Alphen, J., van Beek, E., and Taal, M., 3rd Iinternational Symposium on Flood Defence, Nijmegen, Netherlands, Taylor & Francis/Balkema, ISBN 0415391199. Blain, pp. 373–382, 2006.

Bates, P. D. and De Roo, A. P. J.: A simple raster-based model for flood inumdation simulation, J. Hydrol., 236(1–2), 54–77, 2000.

Chua, L., Merting, F., and Holz, K. P.: River inundation modelling for risk analysis, 1st International Conference on River Basin Management, edited by: Falconer, R. A. and Blain, W. R., pp. 373–382, 2001.

D'alpaos, L., Defina, A., and Mattichio, B.: 2D finite element modeling of flooding due to river bank collapse, Proc. Modeling of Flood Propagation Over Initially Dry Areas, American Society of Civil Engineers (ASCE), edited by: Molinaro, P. and Natale, L., 60–71, 1994.

Han, K. Y., Lee, J. T., and Park, J. H.: Flood inundation analysis resulting from levee break, Journal of Hydraulic Research, International Association for Hydraulic Research (IAHR), 36(5), 747–759, 1998.

Herschy, R. W.: Streamflow measurement, 2nd edition, E & FN Spon, an imprint of Chapman & Hall, UK, 1995.

Huang, S., Rauberg, J., Apel, H., and Lindenschmidt, K.-E.: The effectiveness of polder systems on peak discharge capping of floods along the middle reaches of the Elbe River in Germany, Hydrol. Earth Syst. Sci. Discuss., 4, 211–241, 2007, http://www.hydrol-earth-syst-sci-discuss.net/4/211/2007/.

Lindenschmidt, K.-E., Rauberg, J., and Hesser, F.: Extending uncertainty analysis of a hydrodynamic – water quality modeling system using High Level Architecture (HLA), Water Quality Research Journal of Canada, 40(1), 59–70, 2005.

Lindenschmidt, K.-E., Rauberg, J., and Hohmann, R.: Stofftransport im Fluss- und Auenbereich bei Hochwasser: Quasi-2D hydrodynamische Simulation und Unsicherheitsanalyse, Gas- und Wasserfach: Wasser und Abwasser, 147(11), 720–729, 2006.

Saltelli, A., Chan, K., and Scott, E. M.: Sensitivity analysis, John Wiley & Sons, Ltd., pp. 10, 2000.

Vorogushyn, S., Apel, H., Lindenschmidt, K.-E., and Merz, B.: Coupling 1D hydrodynamic, dike beach and inundation models for large-scale flood risk assessment along the Elbe River, Proceedings for 7th International Conference on Hydroinformatics HIC 2006, Nice, France, 4–8 September 2006, Research Publishing Services, ISBN: 81-903170-2-4, pp. 481–488, 2007.